

Organically Modified Aluminophosphates: Transformation of Boehmite into Nanoparticles and Fibers Containing Aluminodiethylphosphate Tectons

Zbigniew Florjańczyk,^{*,†} Andrzej Wolak,[†] Maciej Dębowski,[†] Andrzej Plichta,[†]
Joanna Ryszkowska,[‡] Janusz Zachara,[†] Andrzej Ostrowski,[†] Ewelina Zawadzak,[‡] and
Magdalena Jurczyk-Kowalska[‡]

Faculty of Chemistry, Warsaw University of Technology, ul. Noakowskiego 3, 00-664 Warszawa, Poland,
and Faculty of Materials Science and Engineering, Warsaw University of Technology, ul. Wołoska 141,
02-507 Warszawa, Poland

Received May 14, 2007. Revised Manuscript Received September 4, 2007

The reaction of boehmite with diethyl phosphoric acid generated in situ in a boiling water solution of triethyl phosphate has been studied in detail. Two kinds of solid products have been isolated and characterized by elemental and XPS analysis, in addition to XRD, TGA, FT-IR, SEM, and MAS NMR techniques. One of them precipitates from the reaction mixture in the form of fibers containing needlelike hexagonal crystals with the unit-cell parameters $a = 21.105(4) \text{ \AA}$ and $c = 9.112(2) \text{ \AA}$ ($V = 3515(1) \text{ \AA}^3$). The crystalline structure comprises hexagonally packed catena $\text{Al}[\text{OP}(\text{O})(\text{OC}_2\text{H}_5)_2]_3$ chains. The other ones form a colloidal dispersion of spherical nanoparticles that consist of a boehmite core covered by aluminodiethylphosphate chains. The NMR studies of the reaction mixture indicate that water soluble aluminophosphate species are also formed in the systems studied. These species are suggested to act as nutrients for the growth of aluminophosphate structures. Colloidal particles and fibers have been included into the polyurethane matrix by in situ polyaddition. The SEM images of the composites surface cross-section shows that spherical nanoparticles are homogeneously distributed in the polymers, whereas fibers tend to agglomerate. Some mechanical reinforcement of the surface of polyurethanes has been accomplished as indicated by the abrasive wear test and AFM images.

Introduction

Aluminophosphate-based materials have been the object of intensive academic and industrial studies with respect to their potential application as catalysts or catalyst supports, reactive fillers in polymeric composites, analytical and industrial adsorbents, flame retardants, flocculation agents, etc.^{1–7} Polymeric structures formed by self-assembly pathways of aluminophosphate species leading to one-dimensional chain, two-dimensional porous layer, and three-dimensional open-framework materials are of special interest.⁴ The starting materials generally employed in the synthesis of aluminophosphate polymers are H_3PO_4 and $\text{Al}(\text{OiPr})_3$ or aluminumoxyhydride in the form of pseudoboehmite. The synthetic procedure typically entails hydrothermal treatment of an aqueous gel in the presence of amine or surfactant as

the template; however, several aluminophosphates of well-defined structures have been also obtained by nonaqueous methods. In some systems, the organic building units were introduced into the framework as coordination ligands by the formation of covalent dative bonds, generating novel structures due to variable linkages between the different subunits. Methyl phosphonic acid^{8–14} and phosphoric acid monoesters^{15–21} have been reported as useful reagents for the preparation of organically modified microporous aluminum phosphonates, aluminophosphate clusters, and mesostructured lamellar aluminophosphates consisting of AlPO_4 layers separated by covalently bonded long alkyl chains.

* To whom correspondence should be addressed. Fax: 48-22-234-7271. E-mail: evala@ch.pw.edu.pl

[†] Faculty of Chemistry, Warsaw University of Technology.

[‡] Faculty of Materials Science and Engineering, University of Warsaw.

(1) Maeda, K.; Mizukami, F. *Catal. Surv. Jpn.* **1999**, *3*, 119.

(2) Corbridge, D. E. C. *Phosphorus 2000*; Elsevier Science B.V.: Amsterdam, 2000.

(3) Szostak, R. *Molecular Sieves: Principles of Synthesis and Identification*; Van Nostrand Reinhold: Toronto, ON, 1989.

(4) Oliver, S.; Kuperman, A.; Ozin, G. A. *Angew. Chem., Int. Ed.* **1998**, *37*, 46.

(5) Mason, M. R. *J. Cluster Sci.* **1998**, *9*, 1.

(6) Martin, E. S.; Wieserman, L. F. U.S. Patent 4 929 589, 1990.

(7) Zygadło-Monikowska, E.; Florjańczyk, Z.; Wolak, A.; Lasota, A.; Plichta, A. Polish patent application P.368877, 2004.

(8) Maeda, K.; Kiyozumi, Y.; Mizukami, F. *Angew. Chem., Int. Ed.* **1994**, *33*, 2335.

(9) Maeda, K.; Akimoto, J.; Kiyozumi, Y.; Mizukami, F. *Angew. Chem., Int. Ed.* **1995**, *34*, 1199.

(10) Maeda, K.; Akimoto, J.; Kiyozumi, Y.; Mizukami, F. *J. Chem. Soc., Chem. Commun.* **1995**, 1033.

(11) Maeda, K.; Hashiguchi, Y.; Kiyozumi, Y.; Mizukami, F. *Bull. Chem. Soc. Jpn.* **1997**, *70*, 345.

(12) Kimura, T. *Chem. Mater.* **2003**, *15*, 3742.

(13) Kimura, T. *Chem. Mater.* **2005**, *17*, 5521.

(14) Kimura, T. *Chem. Mater.* **2005**, *17*, 337.

(15) Fröba, M.; Tiemann, M. *Chem. Mater.* **1998**, *10*, 3475.

(16) Tanaka, H.; Chikazawa, M. *Mater. Res. Bull.* **2000**, *35*, 75.

(17) Schulz, M.; Tiemann, M.; Fröba, M.; Jäger, C. *J. Phys. Chem. B* **2000**, *104*, 10473.

(18) Huang, Y.; Yan, Z. *J. Am. Chem. Soc.* **2005**, *127*, 2731.

(19) Tiemann, M.; Fröba, M. *Chem. Mater.* **2001**, *13*, 3211.

(20) Kimura, T. *Microporous Mesoporous Mater.* **2005**, *77*, 97.

(21) Murugavel, R.; Kuppaswamy, S. *Angew. Chem., Int. Ed.* **2006**, *45*, 7022.

Recently, we have found that the reaction of boehmite with diphenylphosphoric acid (DPP) carried out in boiling xylene leads to the formation of aluminophosphates of fibrous structure, which was attributed to the close-packed hexagonal structure consisting of polymeric chains of catena-Al-(DPP)₃.²² Unfortunately, in this system, we did not succeed in the separation of the fibers from the other products that maintain the boehmite core decorated with aluminophosphates. We have now overcome this problem by using diethyl phosphate (DEP) ligands generated in situ by the controlled hydrolysis of triethyl phosphate (TEP) in the presence of boehmite. In this paper, we report the synthesis and physicochemical characterization of two populations of aluminum phosphate-based materials that are formed in these reactions as well as some preliminary investigations on the utility of these materials as components of polyurethane composites.

Experimental Section

Raw Materials. The starting materials for the synthesis were as follows: pseudo-boehmite (ca. 75 wt % Al₂O₃, Catapal D Alumina, Sasol), TEP (Aldrich, 99%), dextran (Nobiles Ent, 10 kDa), oligo-(ethylene adipate) (OEA, Alfaster T-620 by Alfa Systems Sp. z o.o. Brzeg Dolny), 4,4'-methylenebis(phenyl isocyanate) (MDI, Isonate M 125 by Dow Chemicals), 1,4-butanediol (Aldrich, 99%), ethylene glycol (POCh Gliwice), and glycerol (POCh Gliwice). Listed materials were used as received without further purification.

TEP Hydrolysis. A solution of TEP (3 g, 16.5 mmol) in water (170 mL) was heated under reflux for 48 h, and at defined time intervals, the reaction mixture composition was analyzed. The content of particular phosphoric acid esters was determined on the basis of the intensity of signals in ³¹P NMR spectra ($\delta_{(\text{EtO})_3\text{P}(\text{O})} = 1.49$; $\delta_{(\text{EtO})_2\text{P}(\text{O})\text{OH}} = 2.23$; $\delta_{(\text{EtO})\text{P}(\text{O})(\text{OH})_2} = 1.86$) and titration with 0.1 M aqueous solution of NaOH ($\text{pK}_{(\text{EtO})_2\text{P}(\text{O})\text{OH}} = 5.5$; $\text{pK}_{(\text{EtO})\text{P}(\text{O})(\text{OH})_2} = 9.7$).

Reactions of DEP with Boehmite. A typical synthesis of boehmite modified with DEP proceeded according to the following procedure: boehmite was dispersed in redistilled water followed by the addition of TEP (3-fold molar excess with respect to boehmite). The mixture of substrates was heated under reflux for a required time (from 1 to 48 h). The reaction resulted in the formation (depending on the time of its duration) of a product forming a stable dispersion (**A**) and/or a product isolating in the form of a white precipitate (**B**). Product **B** was isolated by filtration, and product **A** by evaporation of water from the phosphate. The products isolated were washed with acetone and dried at 70–85 °C in air flow.

Synthesis of Polyurethane (PUR) Composites. The synthesis of polyurethanes was carried out by the one-pot method in a vacuum reactor at constant stirring. OEA, MDI, ethylene glycol, and glycerol in 6:9:2:1 mole ratio, respectively, were used as monomers. The following fillers were used for the synthesis of composites: (1) unmodified boehmite, (2) product **A** obtained after 1 h of reaction of boehmite and DEP, and (3) mixture of products **A** and **B** (at 1:1 by weight proportions) resulting from drying of the postreaction mixture obtained after 13 h of reaction of boehmite and DEP. The fillers were dispersed in a mixture of ethylene glycol and glycerol at 120 °C applying a mechanical stirrer. The dispersion process was carried out for 2 h under reduced pressure in order to dehydrate and degas the reaction mixture, followed by a decrease in

temperature to 70 °C, addition of the remaining components and stirring for ca. 15 min. The mixtures obtained were poured into aluminum forms and heated at 120 °C for 16 h.

Elemental Analysis. The hydrogen and carbon contents were determined with using a Perkin-Elmer CHNS/O II 2400 instrument. The aluminum content was determined as follows: the sample was mineralized to conduct all aluminum atoms in the water soluble form of Al³⁺, the ions were next complexed with EDTA and the excess of EDTA was titrated with FeCl₃ solution.

XPS Analysis. The content of heavy elements on the surface of samples was determined by means of an ESCALAB-210 VG Scientific spectrometer equipped with an X-ray radiation source with a double Mg and Al anode (alternatively). The results were evaluated with the use of the ECLIPSE programs.

NMR Spectroscopy. NMR spectra in C₆D₆ or D₂O solutions were obtained on a Varian Mercury 400 MHz spectrometer. Magic angle spinning (MAS) NMR spectra were recorded on Bruker DSX 300 spectrometer at 78.2 (²⁷Al), 121.5 (³¹P), or 75.5 (¹³C) MHz. Chemical shifts are reported relative to external [Al(H₂O)₆]³⁺ (²⁷-Al), 85% H₃PO₄ (³¹P), and TMS (¹³C and ¹H) standards.

FT-IR Spectroscopy. Infrared spectra were collected on a Biorad 165 FT-IR spectrophotometer with the samples in KBr pellets.

Thermogravimetric Analysis (TGA). TGA studies were performed with a Derivatograph Q 1500-D instrument. The samples were heated under flowing dry air at 5–10 °C min⁻¹ up to 1000 °C. TGA ceramic yield (loss on ignition) was used here as an alternative to chemical analysis for most of the solid products obtained.

Particle Size Distribution and ξ Potential. The particle size distribution in the studied dispersions was determined by the photons correlation spectroscopy PCS method, whereas the zeta (ξ) potential of these dispersions was determined on the basis of electrophoresis measurements. Both measurements were carried out with the Zetasizer Nano S ZEN 1600 apparatus (Malvern Instruments Ltd.).

Powder XRD Studies. Laboratory X-ray powder diffraction patterns were recorded on a Seifert HZG-4 automated diffractometer using Cu K α radiation ($\lambda = 1.5418 \text{ \AA}$). The data were collected in the Bragg–Brentano ($\theta/2\theta$) horizontal geometry (flat reflection mode) between 4 and 70° (2θ) in 0.04° steps, at 20 s step⁻¹. The optics of the HZG-4 diffractometer consists of a system of primary Soller slits between the X-ray tube and the fixed aperture slit of 2.0 mm. One scattered-radiation slit of 2 mm was placed after the sample, followed by the detector slit of 0.2 mm.

Microscopy Methods. SEM (scanning electron microscopy) images of the powdered samples were obtained on a LEO 1530 scanning electron microscope. Analysis of the cross-section structure of the composites obtained was performed by the atomic force spectroscopy (AFM) method using a DI multimode with a Nanoscope IIIa driver; the samples were studied by the tapping mode technique.

Density and Specific Surface Studies. The helium density of the samples was determined by means of a helium AccuPyc 1330 pycnometer, whereas the specific surface measurements were performed by the BET method by means of the Gemini 2360 surface analyzer.

PUR Composite Analysis. Density studies of the composites obtained were carried out by means of an electronic type WPA balance, according to the ISO 1183 standard.

Abrasive wear studies were carried out by means of the Schopper–Schlobach type AP 40 apparatus. The mechanical properties at stretching were determined by means of an Instron 1115 testing machine.

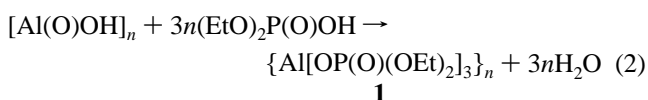
(22) Florjańczyk, Z.; Lasota, A.; Wolak, A.; Zachara, J. *Chem. Mater.* **2006**, *18*, 1995.

on the surface of particles, preventing their agglomeration. The cations might result from the protonation of surface OH groups or Al–O–Al bonds by the phosphoric acid diester.

After about 6 h of reaction, another product starts to isolate in the form of a white powder. After 13 h of reaction, it constitutes about 44 wt % of the products formed, and after 48 h, its content increases to 67 wt %. From now on in this paper, it will be denoted as **B**, whereas the products obtained by concentration of the stable dispersion will be denoted as **A**. These latter ones can be again dispersed to nanoparticles of the size similar to that of particles formed during the reaction, and the dispersion obtained is stable in the pH 2.0–5.8 range. The colloidal systems formed are characterized by relatively high values of zeta potential (40–50 mV), which suggests the formation of an ionic double layer around the particles. It results probably from the partial solubility of products **A** in water, which is indicated by the presence of signals at $\delta = 1.3$ and -4.8 in the ^{27}Al NMR spectrum and at $\delta = 2.7$ in the ^{31}P NMR spectrum of the product **A** dispersion. Product **B**, after separation from products **A** and drying, does not undergo redispersion in water. However, diluted dispersions containing up to ca. 3.5 wt % of the mixture of products **A** and **B** (at a 1:1 weight ratio) can be obtained after several hours of heating in boiling water (see Figures 4D and 5D).

In our previous paper,²² we found that nanoparticles and fibers formed from the reaction of boehmite and diphenylphosphoric acid exhibit a strong tendency for agglomeration and cannot be dispersed in water. It results probably from the hydrophobic properties of aluminum tris(diphenylphosphate), which is formed on the surface of boehmite particles and renders the solvation of these particles by water molecules.

Chemical Structure and Morphology of Product B. Elemental analysis of **B** samples shows that the carbon (~28.8 wt %), hydrogen (5.4 wt %), and aluminum (~5.7 wt %) content do in fact not change during the reaction. On this basis, it can be assumed that aluminum tris(diethyl phosphate) **1**, resulting from the substitution of the hydroxyl group and cleavage of the Al–O–Al bonds in boehmite molecules, is the main component of this phase (eq 2)



In pure **1** ($\text{C}_{12}\text{H}_{30}\text{O}_{12}\text{P}_3\text{Al}$), the carbon, hydrogen, and aluminum content is 29.62, 6.17, and 5.55 wt %, respectively. On the basis of the aluminum and carbon content, it can be estimated that at an average 2.75 DEP ligands fall per 1 aluminum atom in fraction **B**. On the other hand, the average number of ligands bonded to the aluminum atom estimated on the basis of the aluminum and phosphorus content by the ESCA method is equal 2.74, which indicates that the distribution of organic ligands on the surface is the same as in the whole sample. Thermogravimetric analysis shows that product **B** contains about 2.5% absorbed water, which is removed successively during heating up to 220 °C. Thermal decomposition of the product starts above that

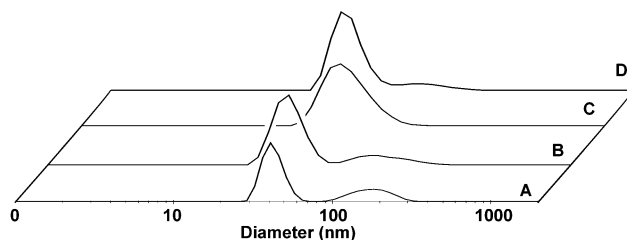


Figure 5. Particle size distribution depending on the volume of particles of (A) **A** after 1 h reaction of TEP and boehmite; (B) **A** after 6 h reaction of TEP and boehmite; (C) **A** after 48 h reaction of TEP and boehmite; (D) mixture of **A** and **B** dispersed after being dried after 13 h reaction of TEP and boehmite.

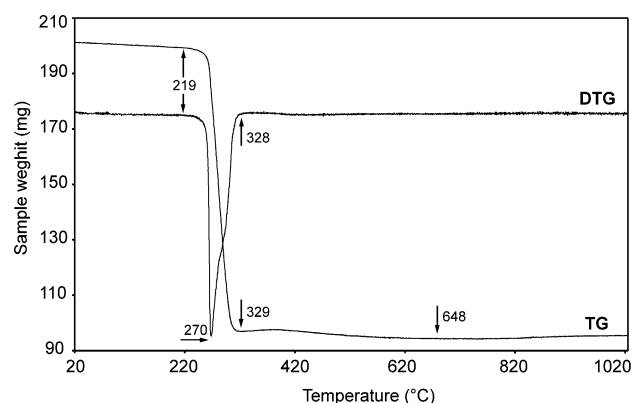


Figure 6. TGA thermogram of product **B**.

temperature. The main mass loss takes place within 220–540 °C (Figure 6).

In view of data on the thermal stability of alkyl phosphates it can be assumed that the decomposition of **1** consists mainly in the elimination of ethylene. The theoretical mass loss for the elimination of six ethylene molecules from compound **1** is 34.6 wt %. At these assumptions the average number of ligands bonded with the aluminum atom can be estimated as 2.8, which is in agreement with the determinations by the elemental analysis and ESCA methods. From 540 to 1000 °C, the mass loss is small, equal to 0.8 wt %. The ceramic yield of the whole process is 64%.

In ^{27}Al NMR MAS spectra of product **B** samples, two signals are present that may be assigned to octahedral aluminum species on the basis of their chemical shifts (Figure 7C). The relatively narrow signal ($W_{1/2}$ 216 Hz) at -26 ppm is attributed to the Al nuclei in **1**. The second signal centered at ca. -3 ppm is quite broad ($W_{1/2}$ \sim 1185 Hz), which suggests that the symmetry of Al nuclei is very low. On the basis of the relative intensity of signals in the ^{27}Al MAS NMR spectrum, it can be estimated that ca. 90% of Al atoms in product **B** exist as **1**.

In the ^{31}P NMR-MAS spectrum of product **B**, one symmetric and narrow ($W_{1/2}$ 171 Hz) signal is present at $\delta \approx -15$ that is accompanied by a set of regularly distributed sidebands (Figure 8C).

Such a structure of the spectrum lets us suppose that there is only one type of phosphorus chemical environment that forms crystallographically equivalent sites. The ^{13}C NMR MAS spectrum, which shows only two sharp signals of ethyl resonance at 18.2 and 63.0 ppm, also supports this supposition. In view of the hitherto studies on the structure of group 13 metals complexes with dialkyl- and diarylphosphate

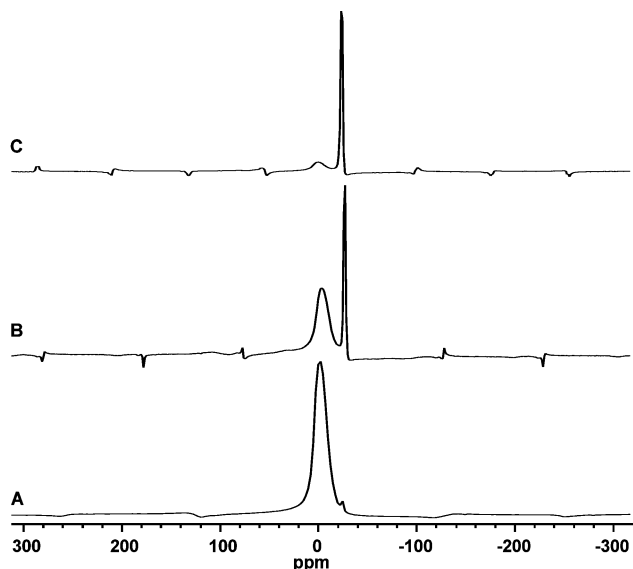


Figure 7. ^{27}Al NMR-MAS spectra: (A) **A** after 1 h; (B) **A** after 48 h; (C) **B**.

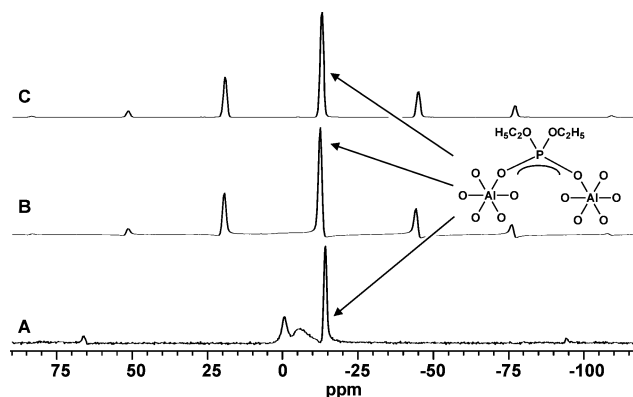


Figure 8. ^{31}P NMR-MAS spectra: (A) **A** after 1 h; (B) **A** after 48 h; (C) **B**.

ligands,²⁵ it can be assumed that the signal observed corresponds to the phosphate groups that bridge between two aluminum atoms. Thus, the octahedral aluminum atoms in **1** are linked to six phosphorus atoms via bridging oxygen, $\text{Al}(\text{OP})_6$.

In the XRD patterns of **B**, a strong reflection at 8.37° 2θ ($d = 10.55 \text{ \AA}$) and a set of less intense reflections in the range of $13\text{--}70^\circ$ 2θ appear (Figure 9E).

On the basis of these reflections, we made an attempt at indexing the XRD pattern (Figure 10). Good matching was obtained for the hexagonal system with the unit-cell parameters $a = 21.105(4) \text{ \AA}$ and $c = 9.112(2) \text{ \AA}$ and the cell volume $V = 3515(1) \text{ \AA}^3$. The widely used criteria for indexing, that is, figures of merit $F_{20} = 47$ (0.0085, 50)²⁶ and $M_{20} = 27$,²⁷ give a high probability of correctness of the solution. To derive possible space groups, all reliable lines available in the pattern were used, and the group $P31c$ with lowest symmetry was assumed. The calculated Bragg reflection positions for this group are presented in Figure 10. Assuming that the mean volume of each non-hydrogen atom in the structure should be close to 20 \AA^3 , the number

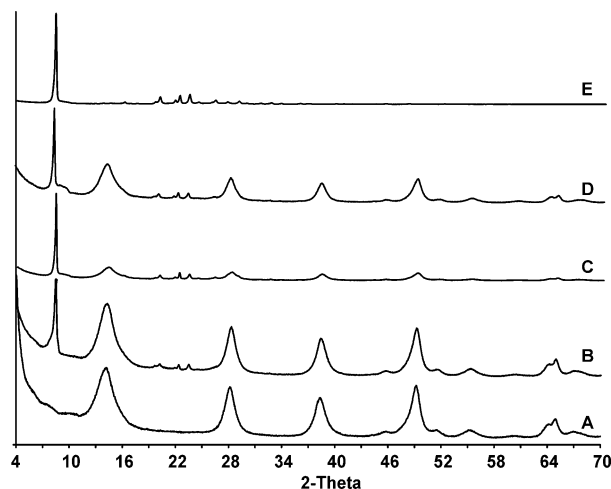


Figure 9. XRD diffractograms: (A) boehmite; (B) **A** after 1 h reaction of TEP and boehmite; (C) **A** after 13 h reaction of TEP and boehmite; (D) **A** after 48 h reaction of TEP and boehmite; (E) **B**.

of molecules of $\text{Al}(\text{DEP})_3$ in the unit cell (Z) is 6 and consistent with the assumed space group.

These results let us suggest that compound **1** possesses a linear structure similar to that of polymeric chains of catenated $\text{Al}(\text{DPP})_3$. The large diffraction peak at $2\theta = 8.37^\circ$ in the XRD pattern is due to the chains arranged in the close-packed hexagonal columnar structure as was schematically depicted in Figure 11. The calculated diameter of the chain ($\sim 12.2 \text{ \AA}$) is slightly lower than that estimated for analogous diphenyl phosphate derivatives (15.1 \AA) and very close to the chain diameters (ca. 12.0 \AA) observed for DEP derivatives of the lanthanides Ce, Pr,²⁸ and Nd,²⁹ which reveal an almost hexagonal packing of chains.

The distance between adjacent Al atoms linked by three phosphate bridges can be estimated as $c/2 = 4.556 \text{ \AA}$. The latter value matches perfectly with the value of the Al \cdots Al separation determined for simple inorganic aluminum phosphate $\text{Al}(\text{H}_2\text{PO}_4)_3$ (4.576 \AA), which forms similar polymeric chains and crystallizes in the $R3c$ space group.³⁰

In product **B**, compound **1** is contaminated by a small amount of another phase of AlO_6 type, which does not give characteristic reflexes in the XRD patterns.

The samples of this material examined by SEM reveal a fibrous structure with the particle size to be in the range $100\text{--}300 \text{ nm}$ in diameter (Figure 12B). These particles are placed irregularly and form a peculiar unwoven fabric. Their specific surface is $27 \text{ m}^2 \text{ g}^{-1}$, and density 1.49 g cm^{-3} . The theoretical density of the crystals of compound **1** is 1.38 g cm^{-3} . These are values considerably smaller than those for the boehmite used ($209 \text{ m}^2 \text{ g}^{-1}$ and 2.71 g cm^{-3} , respectively). Also, more regular and larger agglomerates were obtained by slow water evaporation from diluted dispersions of products **A** and **B** mixtures, to which dextran was additionally introduced. SEM images of the thus obtained material do not show the presence of products **A** agglomerates, but centers of several particles or individual agglomerates of product **B** composed

(25) Mason, M. R. *J. Cluster Sci.* **1998**, *9*, 1.

(26) Smith, G. S.; Snyder, R. L. *J. Appl. Crystallogr.* **1979**, *12*, 60.

(27) de Wolff, P. M. *J. Appl. Crystallogr.* **1968**, *1*, 108.

(28) Han, Y.; Pan, Z.; Shi, N.; Liao, L.; Liu, C.; Wu, G.; Tang, Z.; Xiao, Y. *Wuji Huaxue Xuebao (Chin. J. Inorg. Chem.)* **1990**, *6*, 17.

(29) Lebedev, V. G.; Palkina, K. K.; Maksimova, S. I.; Lebedeva, E. N.; Galaktionova, O. V. *Zh. Neorg. Khim.* **1982**, *27*, 2980.

(30) Kniep, R.; Steffen, M. *Angew. Chem., Int. Ed.* **1978**, *17*, 272.

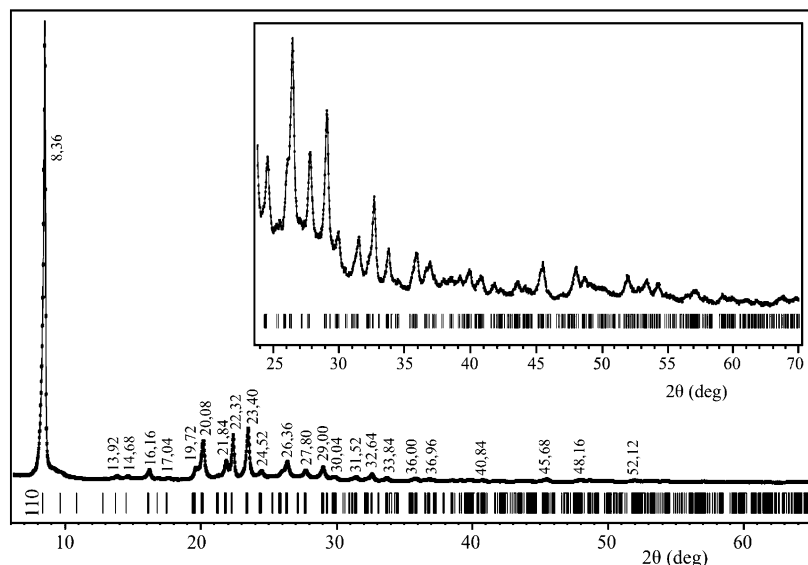


Figure 10. XRD diffractogram of **B**. Theoretical Bragg reflections are derived from the crystallographic system suggested for **B** ($P31c$, $a = 21,105(4)$ Å and $c = 9,112(2)$ Å) and are marked under the axis.

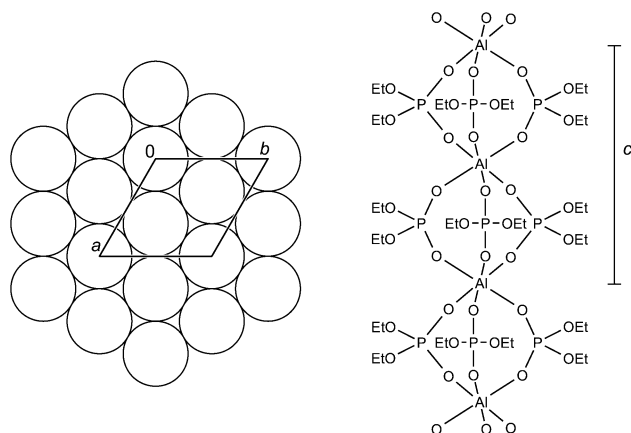


Figure 11. Schematic representation of the structural model of catena-Al-(DEP)₃ (**1**).

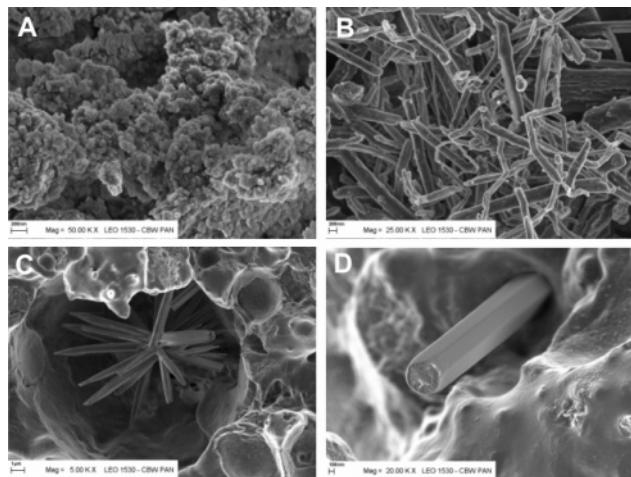


Figure 12. SEM images: (A) **A** after 1 h ($\times 50\,000$); (B) **B** ($\times 25\,000$); (C) **A** and **B** after 13 h in a dextran matrix ($\times 5\,000$); (D) **A** and **B** after 13 h in a dextran matrix ($\times 25\,000$).

of long hexagonal prism (of about 700 nm diameter) and length of several micrometers could be observed (images C and D in Figure 12). For crystals of **1** with $P31c$ symmetry, the hexagonal prismatic habit dominated by the $\{10\bar{1}0\}$ form was predicted using the Bravais–Freidel–Donnay–Harker³¹

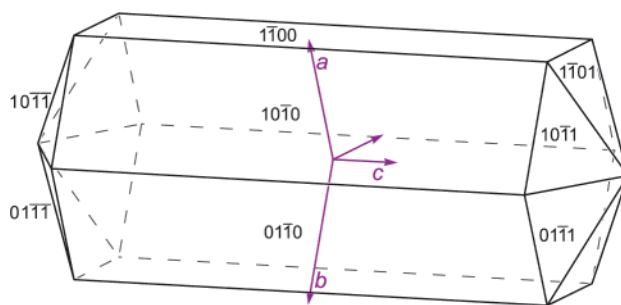


Figure 13. Predicted crystal habit of catena-Al[OP(O)(OEt)₂]₃ in $P31c$ space group according to the Bravais–Freidel–Donnay–Harker law.

analysis (Figure 13). The shape of the filaments is in agreement with the predicted morphology and indicates that compound **1** crystallizes in a chainlike structure in which the intermolecular bonding (van der Waals forces) between adjacent chains (parallel to the $[001]$ directions) are considerably weaker in comparison to the bonds contained within the chains. It results in slow growth perpendicular to the $\{10\bar{1}0\}$ faces.

From among the inorganic aluminum phosphates, a similar structure is shown by $\text{Al}(\text{H}_2\text{PO}_4)_3$, which was isolated by Kniep and Steffen³⁰ in the form of large crystals by evaporation of concentrated acidic solutions of aluminophosphates ($\text{Al}:\text{P} = 1:5$). It suggests that catena type chains of inorganic and organically modified aluminum triphosphates can be formed in solution via self-assembly of aluminum cations and $(\text{HO})_2\text{PO}_2^-$ or $(\text{RO})_2\text{PO}_2^-$ anions, which display a tendency to triple bridge metal centers. To verify this hypothesis, we made an attempt to obtain catena-Al[OP(O)(OC₂H₅)₂]₃ from water-soluble aluminum sources and found that a fibrous material of the same XRD pattern as for product **B** precipitates while heating water solution of aluminum lactate with TEP. In our previous work,²² it was shown that this type of bonding may appear also in aluminum tris(diphenyl phosphate) prepared in anhydrous

(31) (a) Donnay, J. D. M.; Harker, G. *Am. Miner.* **1937**, *22*, 446. (b) Bravais, A. *Etudes Crystallographiques*; Gauthier-Villars: Paris, 1913. (c) Freidel, G. *Bull. Soc. Fr. Mineral.* **1907**, *30*, 326.

Table 1. Carbon and Hydrogen Content in Type A Products

reaction time (h)	elemental analysis of A (%)			OL/Al ratio ^a
	C,	H	Al,	
1	5.1	2.5	31.5	0.09
4	10.6	3.0		
13	12.9	3.6	22.2	0.33
48	20.5	4.3	9.5	1.21

^a OL = organic ligand $-\text{OP}(\text{O})(\text{OC}_2\text{H}_5)_2$.

Table 2. Helium Density and Specific Surface of Boehmite and A and B Products

substance	helium density (g cm^{-3})	specific surface ($\text{m}^2 \text{g}^{-1}$)
boehmite	2.7121	209
product A after 1 h	2.3318	195
product A after 48 h	1.7125	105
product B	1.4919	27

conditions (from aluminum trialkyls and diphenylphosphoric acid); however, in this material, the self-organization of linear chains was disturbed by the presence of nonbridging phosphate units. The reaction with boehmite resulted in the formation of more regular fibrous materials, probably because of the formation of water, which allowed the formation of ionic species.

Chemical Structure and Morphology of Products A.

Elemental and spectroscopic analysis of products A samples collected during the reaction show that in the dispersed nanoparticles, the content of organic substituents increases with time. On the basis of the carbon and aluminum content (Table 1), it can be estimated that after 1 h of reaction, the phosphate ligands constitute ca. 16 wt %, and after 48 h, nearly 65 wt % of product A.

After this time, the composition of the dispersed phase does not change and the average number of organic ligands falling per 1 aluminum atom, determined by elemental analysis, is about 1.2. On the other hand, the ratio of the content of aluminum to phosphorus and carbon atoms determined by the XPS method is 1.0:2.2:8.2, which means that an average of 2.1–2.2 organic ligands fall per 1 aluminum atom in the outer layers of A. XRD patterns of

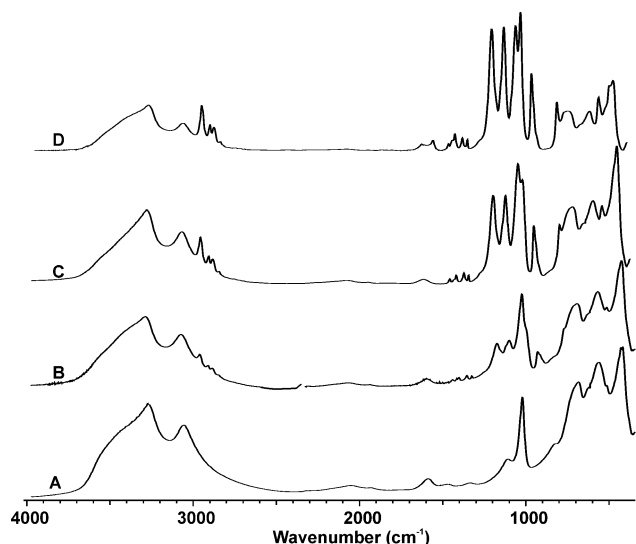


Figure 14. FTIR spectra: (A) boehmite; (B) A after 4 h of TEP and boehmite reaction; (C) A after 13 h of TEP and boehmite reaction A; (D) A after 48 h of TEP and boehmite reaction; (E) B.

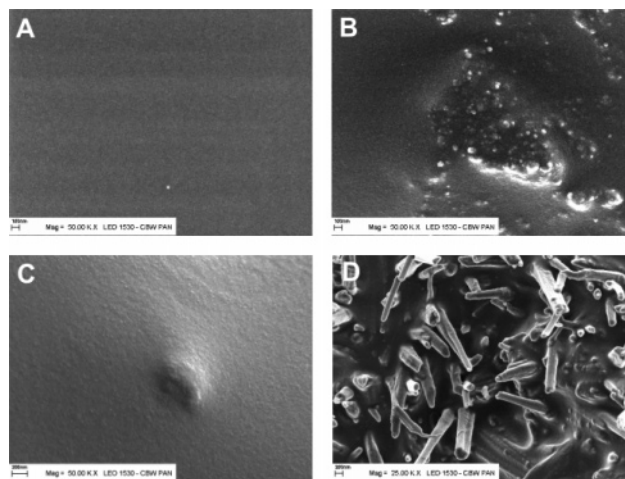


Figure 15. SEM images of the PUR cross section: (A) without filler ($\times 50\,000$); (B) with unmodified boehmite ($\times 50\,000$); (C) with A after 1 h ($\times 50\,000$); (D) with a mixture of A and B ($\times 25\,000$).

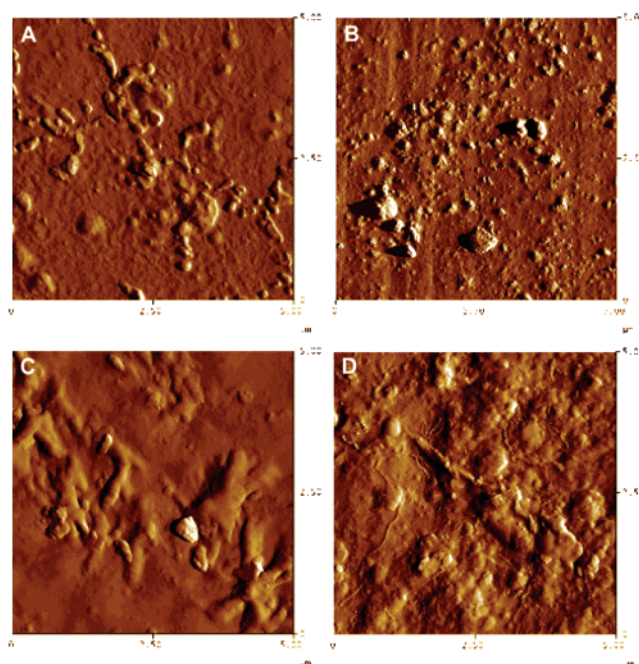


Figure 16. AFM image (picture 2D) of the PUR surface cross-section PUR: (A) without filler; (B) with unmodified boehmite; (C) with product A after 1 h; (D) with a mixture of products A and B.

products A (Figure 9B–D) show that after a short reaction time, an $\text{Al}(\text{OP})_6$ phase already forms, characteristic for compound 1. The intensity of the peaks characteristic for this phase increases at the expense of those of the boehmite phase. It should be noticed, however, that even after a long reaction time, the boehmite phase does not disappear completely (see graphs A and D in Figure 9). An analysis of FT-IR spectra of these products (Figure 14), in which, in addition to signals characteristic of phosphate ligands (main signals 1221, 1146, 1077, and 1046 cm^{-1}), a series of signals is also present that is observed in boehmite spectra and connected with the vibrations of bonds in boehmite (OH stretching vibrations: ν_{as} at 330, ν_{s} at 3072, and Al–O stretching vibrations ν at 674, 615, and 475 cm^{-1}), leads to a similar conclusion.

The presence of signals characteristic for this phase in ^{27}Al (spectra A and B in Figure 7) and ^{31}P NMR MAS spectra

Table 3. Density, Abrasive Wear, Elongation, and Tensile Strength at Break of PUR Composites

PUR material	density (g cm ⁻³)	abrasive wear (mm ³)	elongation at break (%)	tensile strength at break (MPa)
pure PUR	1.2209 ± 0.0034	50.4 ± 3.0	490 ± 22.4	36.8 ± 0.94
PUR + boehmite	1.2456 ± 0.0019	64.3 ± 2.3	580 ± 27.4	42.6 ± 0.60
PUR + A (1 h)	1.2259 ± 0.0030	33.4 ± 1.3	610 ± 41.8	35.0 ± 3.54
PUR + A + B	1.2146 ± 0.0028	33.6 ± 2.8	570 ± 27.4	35.8 ± 3.04

of products **A** (Figure 8) is another premise indicating the formation of the Al(OP)₆ phase. On the basis of the relative intensity of signals at about -3 and -26 ppm in the aluminum resonance spectra, it can be estimated that after 48 h of reaction, about 30% of aluminum atoms in products **A** occurs in the form of Al(OP)₆ phase. The ³¹P spectrum of these products (Figure 8B) is similar to that of product **B**, which means that it contains a singular signal at $\delta \approx -15$ accompanied by several spinning side bands. The ³¹P MAS NMR spectrum of products of small content of organic ligands (ca. 16 wt %, Figure 8A) exhibits two additional signals at ca. -2 and -7 ppm. The structural assignment of these signals is not yet clear. One of the plausible explanations is that they come from DEP or its anions, which are adsorbed on the boehmite surface at the initial stage of reaction and are then transformed into the aluminum phosphate phase.

Taking into account all the hitherto presented experimental data, it is suggested that products **A**, contrary to product **B**, have a gradient structure. The nanoparticles nucleus contains an unreacted boehmite phase, which gradually transforms into regions of greater and greater content of the crystalline Al(OP)₆ phase.

After evaporation of water and organic reagents, the dispersed product **A** nanoparticles form agglomerates (Figure 12A) composed of spherical particles of diameter less than 100 nm. These agglomerates are of a smaller density and smaller specific surface than that of the initial boehmite molecules (Table 2). Both values decrease clearly with an increase in the content of organic substituents in these molecules. This is connected with a decay of the boehmite crystalline phase and formation of considerably larger aggregates than in the initial substrate (average particle size 46 μ m).

Composites of Boehmite and Products A and B with Polyurethanes. Polyurethane matrices were prepared by a one-step method in situ polymerization using poly(ethylene adipate) diol, MDI, ethylene glycol, and glycerol in a 6:9:2:1 molar ratio. Boehmite, product **A**, and the mixture of products **A** and **B** were introduced in the form of a dispersion in ethylene glycol and glycerol. The total concentration of the filler was equal to 3.5 wt %. Samples were formed by casting and then cured at 120 °C for 16 h. SEM images of the surface cross-section of the samples prepared reveal the presence of microfillers in the composites containing unmodified boehmite and product **B** (images B and D in Figure 15).

The shape of **B** fillers is similar to that observed in the dextran matrix. The fillers based on product **A** are hardly seen in these materials (Figure 15C), which suggests that nanoparticles are homogeneously distributed in the organic matrix. In Table 3 are presented the density values and some parameters characterizing the mechanical properties of the composites obtained.

The addition of fillers causes an increase in the maximum elongation at break by about 20%, and in the case of unmodified boehmite, a small increase in tensile strength is observed as well. This latter effect can result from the interaction between the Al-OH groups on the surface of boehmite with urethane groups. (The effect of the boehmite nanoparticles size and concentration on the strength and stiffness of polyurethane composites has been recently described by Karger-Kocsis et al.³²). After introduction of organic groups onto the filler's surface, this effect does not occur. However, the modification of the surface favorably affects the decrease in the abrasion of the composite (by over 50%), whereas the unmodified boehmite does not improve this feature. This is caused by the more uniform distribution of the filler in the polymer matrix and more even surface of composites containing modified boehmite molecules, which is indicated by the AFM spectra of the studied samples surface (Figure 16B-D).

Conclusions

The examination of the reaction products let us suggest that the following phenomena take place during the heating of boehmite in water solution of TEP. Slow hydrolysis of triester yields diethyl phosphoric acid, which reacts with the OH groups linking boehmite layers and breaking Al-O-Al linkages in the mineral. It leads to the formation of a colloidal dispersion of boehmite particles and ionic species produced through gradual dissolution of the mineral structure. Solvated aluminum cations and DEP anions leached into the supernatant act as nutrients for the growth of the catena-Al[OP(O)(OC₂H₅)₂]₃ polymeric chains. In the initial period of reaction, this phase is growing mainly on the surface of boehmite nanoparticles; however, with elapse of time, the nucleation in water solution occurs, which gives rise to the formation of a highly crystalline fibrous structure built of hexagonally packed catena-Al[OP(O)(OC₂H₅)₂]₃ chains doped with small amounts of incorporated Al-O-Al bonds. This phase precipitates from the reaction mixture and therefore both products can be simply separated by filtration.

Nanoparticles containing a boehmite core and aluminophosphate shell after evaporation of water forms agglomerates of micrometric size, which may be again redispersed in water to particles of diameters below 100 nm. These colloidal systems are stabilized by ionic species, which are formed because of the partial solubility of aluminum tris(diethyl phosphate) in water and can be utilized for the formation of nanocomposites with water soluble polymers or hydrophobic polymer latexes. As shown previously, in some systems the addition of 0.5–2.5 wt % of these particles to vinyl polymer latexes leads to a considerable improvement of the mechan-

(32) Gatos, K. G.; Martínez Alcázar, J. G.; Psarras, G. C.; Thomann, R.; Karger-Kocsis, J. *Compos. Sci. Technol.* **2007**, *67*, 157.

ical properties of films obtained from these latexes.³³ In this work, we showed that these particles can also be dispersed in a mixture of ethylene glycol and glycerol and introduced in this form to stiff segments in polyurethanes. Such a modification does not cause improvement in the resistance of polyurethanes to stretching, but very favorably increases the resistance of their surface to abrasiveness. It is also possible to obtain polyurethane composites with a mixture of nanoparticles and fibers, but these latter ones show a strong tendency toward agglomeration in the polymeric matrix.

Although the results of the preliminary studies on the polymer composites are not sufficient to estimate the possibility of their practical application, the fillers based on organically modified aluminophosphates seem to be worth further systematic studies. The synthetic procedure based on hydrolysis of triethyl phosphate in the presence of boehmite is very simple and employs an inexpensive source of the organic ligand. A similar approach can be applied for the synthesis of linear aluminum phosphates decorated with

some other organic groups like CH₃, C₄H₉, ClCH₂CH₂, and CH₃(OCH₂CH₂)_n ($n = 1-7$);^{7,34,35} however, this methodology is limited only to the triesters that exhibit a relatively high rate of hydrolysis. Also, we have observed that pure linear catena type aluminum phosphates can be obtained from aluminum lactate and diethylphosphoric acid by ion-exchange reaction in the water phase. These types of reactions with various kinds of phosphoric acid diesters are currently under study to find the relationship between the structure of organic ligands and the mode of organization of the inorganic core in hybrid aluminophosphates.³⁶

Acknowledgment. The authors gratefully acknowledge the support of the Ministry of Science and Higher Education (4 T09B 001 25; 03/K134/H03/2006). Thanks are also due to Jeffrey Fenton and Sasol North America Inc. for complimentary delivery of boehmite samples.

CM071304O

(33) Florjańczyk, Z.; Dębowski, M.; Wolak, A.; Malesa, M.; Płecha, J. *J. Appl. Polym. Sci.* **2007**, *105*, 80.

(34) Wolak, A. Ph.D. Thesis, Warsaw University of Technology, Warsaw, Poland, 2006.

(35) Florjańczyk, Z.; Lasota, A.; Leśniewska-Mizak, M. *Polimery* **2004**, *49*, 389.

(36) Florjańczyk, Z.; Plichta, A.; Łokaj, K. **2007**, in preparation.